(49) W. H. Dennis, D. H. Rosenblatt, R. R. Richmond, G. A. Finseth, and G. T. Davis, *Tetrahedron Lett.*, **15**, 1821 (1968).
(50) (a) J. P. Martella and W. C. Kaska, *Tetrahedron Lett.*, **47**, 4889 (1968); (b) W. C. Kaska, C. Sutton, and E. Serros, *Chem. Commun.*, 100 (1970).
(51) (a) I. Hashimoto, M. Ryang, and S. Tsutsumi, *Tetrahedron Lett.*, **38**, 3291 (1969); **52**, 4567 (1970); (b) I. Hashimoto, N. Tsuruta, M. Ryang, and S. Tsutsumi, *J. Org. Chem.*, **35**, 3748 (1970).
(52) T. Mizuta, H. Samejima, and T. Kwan, *Bull. Chem. Soc. Jpn.*, **41**, 727 (1968).
(53) (a) M. G. Burnett, *Chem. Commun.*, 507 (1965); (b) D. Bingham and M. G. Burnett, *J. Chem. Soc. A*, 2166 (1970); 1782 (1971).
(54) (a) P. L. Goggin and R. J. Goodfellow, *J. Chem. Soc., Dalton Trans.*, 2355 (1973); (b) P. L. Goggin and J. Mink, *ibid.*, 534 (1974).
(55) "International Tables for X-Ray Crystallography", Kynoch Press, Birmingham, England, 1969.
(56) All computations were carried out on an IBM 360/65. Cell reduction was done with Lawton's TRACER II, and data reduction was done with an extensively modified version of Raymond's UCFACS. In addition to local programs the following were used: NUCLS, Ibers' group least-squares program; Zalkin's FORDAP Fourier program; Coppen's AGNOST for absorption correction; ORFFE, a function and error program by Busing, Martin, and Levy; Johnson's ORTEP2 thermal ellipsoid plotting program.
(57) The programs for refinement of lattice constants and automated operation of the diffractometer are those of Busing and Levy as modified by Picker Corp.
(58) The distances, in mm, of the bounding faces from an arbitrary origin are $d_{100} = 0$, $d_{010} = 0$, $d_{101} = 0$, $d_{0\bar{1}0} = 0.089$, $d_{\bar{1}00} = 0.512$, $d_{10\bar{1}} = 0.047$, $d_{\bar{1}01} = 0.417$, $d_{00\bar{1}} = 0.177$, $d_{001} = 0.115$, $d_{01\bar{1}} = 0.106$, $d_{0\bar{1}1} = 0.117$.
(59) T. C. Furnas, "Single Crystal Orienter Instruction Manual", General Electric Co., Milwaukee, Wis., 1957.
(60) (a) S. Z. Goldberg, C. Kubiak, C. D. Meyer, and R. Eisenberg, *Inorg. Chem.*, **14**, 1650 (1975); (b) S. Z. Goldberg, R. Eisenberg, J. S. Miller, and A. Epstein, submitted for publication in *J. Am. Chem. Soc.*
(61) W. R. Busing and H. A. Levy, *J. Chem. Phys.*, **26**, 563 (1957).
(62) (a) J. De Meulenaer and H. Tompa, *Acta Crystallogr.*, **19**, 1014 (1965); (b) L. K. Templeton and D. H. Templeton, Abstracts, American Crystallographic Association Meeting, Storrs, Conn., 1973, No. E10.
(63) D. T. Cromer and B. Mann, *Acta Crystallogr., Sect. A*, **24**, 321 (1968).
(64) D. T. Cromer, *Acta Crystallogr.*, **18**, 17 (1965).
(65) $R_1 = \sum||F_o| - |F_c||/\sum|F_o|$; $R_2 = [\sum w(|F_o| - |F_c|)^2/w|F_o|^2]^{1/2}$; estimated standard deviation of an observation of unit weight is $[\sum w(|F_o| - |F_c|)^2/(N_o - N_v)]^{1/2}$ where N_o and N_v are the number of observations and variables, respectively.
(66) M–C bonds were lengthened by ~0.03 Å but Pd(2)–C(6) was shortened by 0.003 Å and Pd(2)–C(4) was lengthened by only 0.008 Å. C–N and N–Me bonds were shortened by 0.01–0.04 Å.
(67) Supplementary material.
(68) J. Donohue, "The Structures of the Elements", Wiley, New York, N.Y., 1974, p 216.
(69) (a) L. D. Brown, K. N. Raymond, and S. Z. Goldberg, *J. Am. Chem. Soc.*, **94**, 7664 (1972); (b) G. L. Simon, A. W. Adamson, and L. F. Dahl, *ibid.*, **94**, 7654 (1972).
(70) F. A. Cotton, T. G. Dunne, and J. S. Wood, *Inorg. Chem.*, **3**, 1495 (1964).
(71) (a) L. F. Dahl and R. E. Rundle, *Acta Crystallogr.*, **16**, 419 (1963); (b) M. F. Bailey and L. F. Dahl, *Inorg. Chem.*, **4**, 1140 (1965); (c) L. F. Dahl, E. Ishishi, and R. E. Rundle, *J. Chem. Phys.*, **26**, 1750 (1957); (d) L. B. Handy, J. K. Ruff, and L. F. Dahl, *J. Am. Chem. Soc.*, **92**, 7312 (1970).
(72) (a) W. M. Butler and J. H. Enemark, *Inorg. Chem.*, **12**, 540 (1973); (b) W. M. Butler, J. H. Enemark, J. Parks and A. L. Balch, *ibid.*, **12**, 451 (1973).
(73) (a) B. Jovanovic and Lj. Manojlovic-Muir, *J. Chem. Soc., Dalton, Trans.*, 1176 (1972); (b) B. Jovanovic, Lj. Manojlovic-Muir, and K. W. Muir, *ibid.*, 1178 (1972).
(74) M. Elian and R. Hoffmann, *Inorg. Chem.*, **14**, 1058 (1975).
(75) S. Z. Goldberg, R. Eisenberg, and J. Miller, to be submitted for publication.
(76) M. D. Vaira and A. B. Orlandini, *Inorg. Chem.*, **12**, 1292 (1973).
(77) M. E. Gress and R. A. Jacobson, *Inorg. Chem.*, **12**, 1746 (1973).
(78) B. W. Davies and N. C. Payne, *Can. J. Chem.*, **51**, 3477 (1973).
(79) (a) R. Nast and W. Pfab, *Naturwissenschaften*, **39**, 300 (1952); (b) W. Pfab and R. Nast, *Z. Kristallogr., Kristallgeom., Kristallphys., Kristallchem.*, **111**, 259 (1959).
(80) M. A. El-Sayed and R. K. Sheline, *J. Am. Chem. Soc.*, **78**, 702 (1956).
(81) (a) W. P. Griffith and G. Wilkinson, *J. Inorg. Nucl. Chem.*, **7**, 295 (1958); (b) W. P. Griffith and A. J. Wickham, *J. Chem. Soc. A*, 834 (1969).
(82) H. Isci and W. R. Mason, *Inorg. Chem.*, **14**, 913 (1975).
(83) A. L. Balch, personal communication.
(84) **Note Added in Proof.** The crystal and molecular structure of $[(n\text{-}Pr)_4N]_2[Pt_2Cl_4(CO)_2]$ has recently been reported [A. Modinos and P. Woodward, *J. Chem. Soc., Dalton Trans.*, 1516 (1975)]. The structure of the anion is similar to that reported here except the two coordination planes have a dihedral angle of ca. 60° between them.

Contribution from the Departments of Chemistry, The Ohio State University, Columbus, Ohio 43210, and Texas A&M University, College Station, Texas

Preparation and Nuclear Magnetic Resonance Studies of Stereochemically Nonrigid Magnesium, Zinc, and Cadmium Derivatives of Hexaborane(10). Crystal and Molecular Structure of $Mg(THF)_2(B_6H_9)_2$[1]

D. L. DENTON, W. R. CLAYTON, M. MANGION, S. G. SHORE,* and EDWARD A. MEYERS

Received July 18, 1975 AIC50515T

Hexaborane(10) has been deprotonated by methylmagnesium halides and the dimethyl derivatives of magnesium, zinc, and cadmium to form a new series of metalloboranes: $Mg(THF)_2(B_6H_9)_2$, $Zn(THF)_2(B_6H_9)_2$, and $Cd(B_6H_9)_2$ which were isolated as crystalline solids. Variable-temperature ^1H NMR spectra of these compounds indicate that they are stereochemically nonrigid with bridging hydrogens and metal being involved in the dynamic processes. At low temperatures the spectra are consistent with metal insertion into a basal boron–boron bond of the anion. The crystal and molecular structure of $Mg(THF)_2(B_6H_9)_2$ has been determined. Each $B_6H_9^-$ anion is coordinated to magnesium through one of its two nonadjacent basal boron–boron bonds. Three-dimensional x-ray data were collected on an automated diffractometer with monochromatized Mo Kα radiation. The structure was solved in the space group $P4_12_12$ with four molecules in the unit cell for which $a = 11.20$ (1), $c = 16.52$ (2) Å (−70°); $a = 11.38$ (1), $c = 16.42$ (2) Å (22°). The calculated densities are 1.02 and 0.99 g/cm^3, respectively. The structure was refined by full-matrix least squares to a final conventional R index of 0.055 for 482 unique reflections with $I \geq 3\sigma(I)$ obtained at −70°. The Mg–B distances are 2.38 (1) and 2.48 (1) Å, and the Mg–O bond distance is 2.019 (5) Å. Bond distances and angles within the B_6H_9 and THF units appear normal; the THF rings are distorted from planarity.

Introduction

The Bronsted acidity of hexaborane(10) is well established and several nonahydrohexaborate(1−) salts have been isolated.[2-5] Deprotonation of B_6H_{10} has been shown to occur by the removal of a bridging proton from one of the four B–H–B bridges. Boron-11 and ^1H NMR spectra of the $B_6H_9^-$ anion in solution suggest rapid exchange of the three remaining bridge hydrogens on the ^1H NMR and boron-11 NMR time scales[3,6] (Similar rapid exchange of the bridge protons in hexaborane(10) has recently been established.[7]) However, the solid-state structure of the nonahydrohexaborate(1−) anion has remained unknown.

The only reported metalloborane involving the nonahydrohexaborate(1−) anion is $[(C_6H_5)_3P]_2CuB_6H_9$.[8] Spectral evidence suggested that the copper had been inserted into a basal boron–boron bond of the anion.

* To whom correspondence should be addressed at The Ohio State University.

We report the preparation, characterization, and NMR studies of magnesium, zinc, and cadmium derivatives obtained directly by the deprotonation of hexaborane(10). We also present the molecular structure of $Mg(THF)_2(B_6H_9)_2$.

Experimental Section

Starting Materials. Pentaborane(9) and diborane were purchased from the Callery Chemical Co. and used as received. Hexaborane(10) was prepared by reaction of diborane with $K(1\text{-}BrB_5H_7)$.[9] Synthesis of $2\text{-}CH_3B_6H_9$ was by a similar method. Methyl bromide from the Matheson Co. was used to prepare Grignard solutions. Dimethylmagnesium was obtained by the addition of anhydrous dioxane to a solution of methylmagnesium bromide.[10]

The active methyl concentration was determined by methanolysis, the magnesium content was checked by EDTA titration, and the absence of bromide was confirmed by potentiometric titration. Dimethylzinc was prepared by the disproportionation of methylzinc iodide produced by the reaction of methyl iodide with a zinc–copper couple.[11] Dimethylcadmium was formed by the addition of anhydrous cadmium chloride (J. T. Baker) to an ether solution of methyllithium from the Foote Mineral Co.[12] Hydrogen chloride was obtained from the Matheson Co. Methylene-d_2 chloride and tetrahydrofuran-d_8 were purchased from Mallinckrodt Nuclear Co. Dimethyl-d_6 ether was prepared from the reaction of $KOCD_3$ with CD_3I in THF. Methanol-d_4 and methyl-d_3 iodide were purchased from Stohler Isotopes Co. All solvents were distilled from $LiAlH_4$ and stored under vacuum.

Apparatus. All manipulations were carried out on a standard high vacuum line or in a glovebox under an atmosphere of dry pure nitrogen. Proton magnetic resonance spectra were obtained at 100 MHz and boron-11 NMR spectra were obtained at 32.1 MHz using a Varian high-resolution HA-100 spectrometer. Heteronuclear decoupling was accomplished by means of assessories which have been previously described.[7] Chemical shifts for boron-11 NMR spectra were measured relative to an external BCl_3 standard (δ −46.8 ppm) or $B(CH_3)_3$ sample (δ −86.0 ppm) and are reported relative to $BF_3{\cdot}O(C_2H_5)_2$. ^1H NMR spectra were run using benzene, chloroform, or methylene chloride as the lock signal. Chemical shifts are reported relative to $Si(CH_3)_4$ using a value of τ 2.734 for benzene, τ 2.75 for $CHCl_3$, and τ 4.67 for CH_2Cl_2. Peak areas were measured with a polar planimeter. Where appropriate, corrections for boron-decoupled spectra were applied to compensate for hydrogens coupled to boron-10 ($I = {}^5/_2$). Corrections were not required for "thermally decoupled" spectra as relaxation times are at least as short for boron-10 as boron-11.[13] Infrared spectra were obtained on a Perkin-Elmer 457 spectrophotometer using KBr windows. All spectra of solids were obtained as Nujol mulls. Absorptions masked by Nujol were observed from mulls in hexachlorobutadiene.

Analytical Procedures. Standard analytical techniques were used to determine B, Mg, Zn, Cd, active H, and CH_3. Details are presented elsewhere.[1]

Reactions of B_6H_{10} with $Mg(CH_3)_2$. In a nitrogen-filled glovebox, 1.00 ml of 0.428 M $Mg(CH_3)_2$ in THF was syringed into a reaction bulb which was fitted to a vacuum-line extractor. On the vacuum line the solution was frozen to −196°. The extractor was evacuated, and 0.85 mmol of B_6H_{10} was condensed into the bulb. The bulb was warmed to −78°. The walls of the vessel were warmed above −78° briefly to allow the frozen hexaborane(10) to melt into the solution. Rapid methane evolution commenced immediately accompanied by the precipitation of a white solid. The mixture was stirred at −78° until the gas evolution had nearly ceased (15 min). The mixture was cooled to −196° and the evolved methane was measured to be 0.431 mmol. Upon warming the vessel to 0° gas evolution resumed at a rapid rate. In 15 min an additional 0.419 mmol of methane was produced. Thus, the total amount of gas evolved was 0.85 mmol. About 10 ml of THF was condensed on the "dry" white solid to form a slurry. The extractor was then inverted to filter the solid, which was washed several times with THF. The product was then dried under high vacuum at room temperature for several days. Drying times were reduced to several hours by heating to 65° without noticeable decomposition; yield 95%. Infrared spectrum of $Mg(THF)_2(B_6H_9)_2$ as a mull (cm^{-1}): 2993 (m), 2905 (m), 2580 (s), 2540 (s), 2490 (s), 1990 (w, br), 1890 (w, br), 1790 (w, br), 1448 (m), 1407 (m), 1349 (m), 1250 (m, br), 1180 (w), 1065 (m, sh), 1058 (m), 1041 (m), 1010 (s), 956 (m), 915 (m), 872 (s), 861 (s), 830 (m), 800 (m), 770 (m), 714 (m), 690 (w), 623 (m), 597 (m), 569 (w). Anal. Calcd for $Mg(B_6H_9)_2{\cdot}2.2THF$: B, 39.2; Mg, 7.35; mmol of H_2/mmol of sample, 28.0. Found: B, 38.3; Mg, 7.44; mmol of H_2/mmol of sample, 27.5.

In an attempt to isolate $CH_3MgB_6H_9$ 2.0 ml of a 0.35 M THF solution of dimethylmagnesium was allowed to react with 0.70 mmol of B_6H_{10} at −78° in a procedure similar to that described above. The evolved methane was measured to ensure complete reaction. During the washing of the white solid product the temperature never exceeded 0°. The x-ray powder pattern,[1] infrared spectrum, and elemental analysis of the isolated product were the same as those of $Mg(THF)_2(B_6H_9)_2$. Stirring a sample of the solid in HCl(l) at −111° evolved only a trace of CH_4. However, methanolysis of the THF-soluble material washed from the solid in the extraction generated 0.64 mmol of CH_4.

Reaction of CH_3MgX with B_6H_{10}. In a procedure similar to that described for the reaction with dimethylmagnesium, 1.0 ml of a 1.50 M THF solution of CH_3MgBr was allowed to react with 1.5 mmol of B_6H_{10}. The reaction proceded rapidly at −78° to generate a quantitative yield of CH_4 and a white precipitate which was isolated. The solid appeared to be a mixture of $Mg(THF)_2(B_6H_9)_2$ and a solvate of $MgBr_2$. The reaction of B_6H_{10} with CH_3MgBr or CH_3MgI in diethyl ether proceeded more slowly and produced an ether-soluble colorless oil. Addition of THF to the ether solutions precipitated $Mg(B_6H_9)_2{\cdot}2THF$. Anal. Calcd for $Mg(B_6H_9)Br{\cdot}1.7THF$: Mg, 7.90; B, 21.1; mmol of H_2/mmol of sample, 14.0. Found: Mg, 7.84; B, 20.2; mmol of H_2/mmol of sample, 14.2. The infrared spectrum was identical with that of $Mg(THF)_2(B_6H_9)_2$ and the x-ray powder pattern[1] contained all of the lines assigned to it plus some unidentified lines.

Reaction of $Zn(CH_3)_2$ with B_6H_{10}. In a typical reaction 1.0 mmol of $Zn(CH_3)_2$ and 1.0 mmol of B_6H_{10} were condensed into a reaction tube on a vacuum-line extractor containing 0.1 ml of THF. The solution was then warmed to 0° and stirred vigorously. After 1 h about 0.85 mmol of CH_4 had been evolved. Generally, the reaction rate had significantly decreased at this point and decomposition had begun so the reaction was stopped. If allowed to continue, the reaction would generate the total amount of methane expected, but the solution would turn yellow-green and contain bits of metallic zinc. Upon termination of the reaction excess hexaborane(10) and dimethylzinc were distilled from the reaction vessel. A viscous yellow oil remained in the tube which was dissolved in chloroform. Diethyl ether was added to precipitate a white solid and the volatiles were distilled off. The product was again precipitated from chloroform with ether, filtered, washed, and dried; yield of $Zn(THF)_2(B_6H_9)_2$ 50%. Infrared spectrum of $Zn(B_6H_9)_2{\cdot}2THF$ as a mull (cm^{-1}): 2992 (m), 2905 (m), 2587 (s), 2540 (vs), 2520 (sh), 1960 (vw, br), 1920 (w, br), 1880 (vw, br), 1448 (s), 1385 (m), 1348 (w), 1312 (w), 1300 (w), 1262 (w), 1248 (w), 1178 (w), 1070 (m), 1038 (m), 1018 (s), 973 (m), 914 (m), 860 (s, br), 795 (sh), 787 (m), 765 (m), 710 (m), 627 (m), 610 (m), 585 (m), 561 (w). Anal. Calcd for $Zn(B_6H_9)_2{\cdot}2THF$: Zn, 17.6; B, 34.8; mmol of H_2/mmol of sample, 28.0. Found: Zn, 17.8, B, 34.6; mmol of H_2/mmol of sample, 28.6.

Reaction of $Cd(CH_3)_2$ with B_6H_{10}. Under vacuum 1.50 mmol of B_6H_{10} was dissolved in 0.15 ml of THF in the reaction tube of an extractor. At −196°, 1.50 mmol of $Cd(CH_3)_2$ was condensed into the vessel. The solution was warmed to 6.5° to allow a moderate reaction rate with minimum decomposition. The solution was protected from light as the product appeared to be light sensitive. Two and one-half hours was required for 1.2 mmol of methane to be evolved. If allowed to continue, the reaction proceeded to 95% completion but was accompanied by considerable decomposition including the deposition of metallic cadmium. Generally after 75% of the methane was produced, all volatiles were distilled from the solution which left some white solid in a yellow oil. About 5 ml of chloroform was then added, followed by an equal volume of ether or pentane. Shielded from light, the solution was filtered in the extractor and the white product was washed and dried; yield of $Cd(B_6H_9)_2$ 35%. Infrared spectrum of $Cd(B_6H_9)_2$ indicated the presence of a small amount of coordinated THF (cm^{-1}): 2960 (w), 2910 (w), 2880 (w), 2620 (m), 2610 (s), 2575 (s), 2565 (s), 2545 (s), 1940 (w, br), 1830 (w, br), 1500 (m), 1440 (w), 1420 (w), 1021 (m), 1003 (s), 860 (w), 818 (w), 790 (m), 755 (w), 718 (m), 680 (w), 623 (m), 602 (m), 560 (w). Anal. Calcd for $Cd(B_6H_9)_2{\cdot}0.2THF$: Cd, 41.0; B, 47.2; mmol of H_2/mmol of sample, 28.0. Found: Cd, 41.5; B, 45.2; mmol of H_2/mmol of sample, 28.2.

Reaction of B_5H_9 with CH_3MgBr. On the vacuum line 4.00 ml

of 0.90 M CH_3MgBr solution in THF was frozen to −196° and 5.64 mmol of B_5H_9 was condensed into the vessel. The solution was allowed to warm slowly. Methane evolution commenced at −35°, but a more convenient reaction rate was obtained at −23°. Initially the solution remained clear, but after several minutes a heavy white precipitate formed (After 3 h the temperature was raised to 0° and finally to room temperature for 1 h.) A total of 2.35 mmol of methane was evolved which represents 65% reaction based on the Grignard used. The volatiles, unreacted B_5H_9 and THF, were identified by their infrared spectra. They were condensed into a vessel containing an excess of potassium hydride. Upon warming, the pentaborane(9) reacted with the KH to yield 1.38 mmol of hydrogen. Thus the ratio of the CH_4 evolved per B_5H_9 consumed in the reaction was 1.0/1.8. Addition of an aqueous alkaline solution of excess $(CH_3)_4NCl$ to the reaction mixture gave the metathesis product $(CH_3)_4NB_9H_{14}$ as identified by its infrared spectrum and x-ray powder diffraction pattern.[3] An 80% yield of $(CH_3)_4NB_9H_{14}$ was obtained based on the amount of pentaborane(9) consumed in the reaction. In reactions where the B_5H_9:CH_3MgBr ratio was adjusted to 2:1, 80% reaction occurred based on the CH_4 evolved. The boron-11 NMR spectrum showed $B_9H_{14}^-$ to be the only detectable product.

X-Ray Structure Determination of $Mg(THF)_2(B_6H_9)_2$. Single crystals of $Mg(THF)_2(B_6H_9)_2$ were grown from a CH_2Cl_2 solution at about −45° and were sealed at room temperature under dry N_2 in thin-walled glass capillaries. Preliminary precession and Weissenberg photographs showed the unit cell to be tetragonal. Systematic extinctions ([$h00$], $h \neq 2n$; [$00l$], $l \neq 4n$) are unique for the enantiomorphic space groups $P4_12_12$ and $P4_32_12$. From single-crystal diffractometry cell dimensions were obtained at two temperatures: a = 11.20 (1), c = 16.52 (2) Å (−70°); a = 11.38 (1), c = 16.42 (2) Å (room temperature). An assumed Z = 4 $Mg(THF)_2(B_6H_9)_2$ gave d_{calcd} = 1.02 g/cm³ (−70°) and 0.99 g/cm³ (room temperature).

The primary data set which was used for the final solution of the structure was obtained at −70°. The cell dimensions and an orientation matrix for the data collection at −70° were determined by least-squares refinement of the setting angles of 19 carefully measured reflections well centered on a computer-controlled Picker FACS-III four-circle diffractometer using Mo Kα radiation (λ 0.7107 Å) monochromatized by reflection from the (002) plane of an oriented graphite monochromator ($2\theta_{mon}$ = 11.69°). The diffractometer was equipped with an Enraf Nonius temperature controller. Intensity data were collected from a crystal with approximate dimensions of 0.11 × 0.12 × 0.20 mm. Integrated intensities were obtained by a θ–2θ scan technique, scanning the Kα peaks symmetrically for 2.4° at a rate of 2°/min. Stationary-background counts for 10 s were obtained. (The standard reflections were measured periodically and showed no significant variation with time.) The intensity data were corrected for background and standard deviations were assigned as described previously[14] using a value of 0.05 for ρ. Intensities were corrected for Lorentz and polarization effects, but no corrections for absorption or extinction were applied. Of the 1769 unique reflections ($h \leq k$) which were collected to a maximum $(\sin\theta)/\lambda$ = 0.700, 502 had $I \geq 3\sigma(I)$ and were considered observed for purposes of subsequent structure refinement.

An initial data set on another crystal was obtained at room temperature. However, reflections could not be observed beyond $(\sin\theta)/\lambda$ = 0.35 and only 84 of the observed reflections had $I \geq 3\sigma(I)$. This data set was used in the preliminary stages of solving the structure until the low-temperature data set became available. These 84 observed reflections were used to obtain a Patterson map. Magnesium was located at the special position (x, x, 0) where x = 0.02. The magnesium–oxygen vector was found to be (0, ±0.14, ±0.06). This leads to four nonequivalent oxygen positions: A (0.02, 0.16, 0.06); B (0.02, 0.16, −0.06); C (0.02, −0.12, 0.06); D (0.02, −0.12, −0.06). Fourier maps failed to show any other structural details; however, four carbon atoms can be placed in the unit cell cooresponding to a planar approximation of the THF structure. A nontrivial assumption is made that the THF structure is mirrored across the plane (Figure 1) defined by magnesium, oxygen, and the point midway between C(2) and C(3). The position of the THF ring can then be described in terms of two angles τ, the angular tilt of the THF plane from the Mg–O vector, and ϕ, the rotation around the Mg–O vector and various positions calculated for the carbon atoms. An R factor was calculated for various values of ϕ and τ and the minimum R was assumed to reflect the best THF position. A minimum value of R = 0.36 was obtained for each of the four possible oxygen positions.

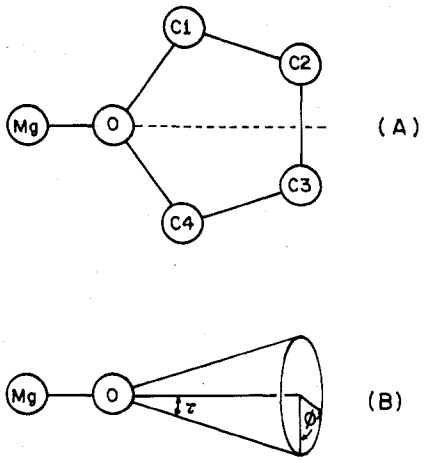

Figure 1. (A) THF ring bound to Mg. (B) Orientation angles for the THF ring with respect to the Mg–O vector.

When low-temperature data became available, the four trial structures obtained were tried in least-squares refinement[15] in the space group $P4_12_12$. The correct model gave R = 0.24 compared to the other models with R's of 0.30. A Fourier map showed the location of the hexaborane framework. Anisotropic refinement using unit weights converged at R = 0.12. A conventional difference synthesis failed to show any hydrogen atom locations. However, a weighted difference map, using the weighting scheme of Clayton, Mangion, and Meyers,[16] showed the positions of 15 of the 17 hydrogen atoms. Final refinement was made with anisotropic temperature factors for the heavy atoms and fixed isotropic temperature factors (U = 0.080) for hydrogen atoms. Hydrogen atoms bonded to carbon were fixed at calculated tetrahedral positions 0.98 Å from carbons. It was necessary to constrain $U_{11} = U_{22}$ for atom C(2) due to layer interactions and divergence of the two parameters during least-squares refinement. Twenty high-angle reflections were removed from the fixed least-squares data set due to extreme disagreement. Each of these points calculated F_c close to zero. (The most common reason for this disagreement is uneveness in the response across the face of the scintillation detector. This does not seem to be the case here, but other mechanical and electronic difficulties had been experienced with the diffractometer used.) The structure was refined to a final conventional R = 0.055 and a final weighted R = 0.054 where the weight $w = 1/[\sigma^2(I) + 0.5I]^{1/2}$. The standard error in an observation of unit weight, Σ, was Σ = 1.35. Refinement was terminated when the calculated shifts were less than one-fourth of the estimated standard deviations. Atomic scattering factors for magnesium, oxygen, and carbon were from Cromer and Waber.[17] The atomic scattering factor tables for hydrogen were those of Stewart, Davidson, and Simpson.[18]

An attempt was made to determine whether the space group was $P4_12_12$ or $P4_32_12$. Anomalous dispersion terms were estimated for the light atoms by extrapolation from the values of Cromer[17] ($\Delta\chi'$, $\Delta\chi''$ values: Mg, 0.05, 0.05; O, 0.016, 0.006; C, 0.008, 0.002; B, 0.006, 0.001). Least-squares refinement for both space groups converged to identical R values, bond angles, and distances.[20] Thus it was not possible to differentiate between the two space groups.

Results and Discussion

Crystal and Molecular Structure of $Mg(THF)_2(B_6H_9)_2$. Positional and thermal parameters based on space group $P4_12_12$ are listed in Tables I and II. No abnormally short nonbonded contact distances between molecules are observed. The distances between nonhydrogen atoms belonging to different molecules all exceed 3.92 Å.

Figure 2 provides a view of the molecular structure of $Mg(THF)_2(B_6H_9)_2$ showing thermal motion ellipsoids.[21] Figure 3 is a stereoscopic view of the $Mg(THF)_2(B_6H_9)_2$ structure. Selected bond distances and bond angles are provided in Tables III and IV. (Note that the asymmetric unit contains one Mg, one THF, and one B_6H_9.) The $Mg(THF)_2(B_6H_9)_2$ molecule has C_2 symmetry. The B_6 framework is a pentagonal pyramid in which the apical boron lies 0.96 Å above the plane of the basal borons. The bo-

Table I. Fractional Coordinates and Thermal Parameters for $Mg(THF)_2(B_6H_9)_2$[a]

Atom	10^4x	10^4y	10^4z	U_{11}	U_{22}	U_{33}	U_{12}	U_{13}	U_{23}
Mg1	160 (2)	160 (0)	0 (0)	299 (16)	299 (0)	339 (18)	−12 (21)	55 (13)	−55 (0)
O1	−120 (5)	−1297 (4)	694 (3)	508 (41)	273 (33)	323 (33)	−11 (34)	56 (32)	−5 (25)
C1	−121 (9)	−1319 (8)	1572 (4)	818 (78)	464 (61)	384 (53)	−12 (66)	50 (61)	122 (47)
C2	−534 (9)	−2564 (10)	1795 (6)	892 (63)	892 (0)	502 (65)	74 (72)	178 (63)	180 (69)
C3	−1006 (10)	−3075 (9)	1041 (8)	876 (88)	407 (71)	898 (84)	−27 (65)	−32 (81)	23 (64)
C4	−322 (8)	−2490 (8)	382 (5)	598 (72)	361 (58)	447 (50)	−149 (54)	20 (53)	−173 (46)
B1	197 (9)	2440 (9)	1703 (5)	372 (69)	516 (73)	283 (56)	127 (62)	−62 (55)	−75 (55)
B2	665 (11)	3898 (10)	1405 (8)	704 (90)	213 (66)	671 (81)	−47 (62)	−223 (75)	−52 (66)
B3	1637 (12)	2847 (11)	1375 (6)	774 (96)	518 (85)	433 (75)	−144 (73)	−164 (75)	−56 (69)
B4	987 (9)	1517 (11)	1043 (7)	377 (73)	401 (79)	457 (61)	−9 (56)	−39 (56)	−50 (59)
B5	−462 (9)	1766 (10)	846 (6)	438 (83)	363 (76)	273 (58)	103 (51)	−60 (58)	−124 (50)
B6	−692 (9)	3286 (10)	1069 (7)	712 (85)	378 (75)	286 (62)	105 (63)	67 (60)	37 (56)

[a] The complete temperature factor expression is $\exp\{-2\pi^2(a^{*2}U_{11}h^2 + b^{*2}U_{22}k^2 + c^{*}U_{33}l^2 + 2a^{*}b^{*}U_{12}hk + 2a^{*}c^{*}U_{13}hl + 2b^{*}c^{*}U_{23}kl)\}$.

Table II. Fractional Coordinates for Hydrogen Atoms of $Mg(THF)_2(B_6H_9)_2$[a]

Atom	10^3x	10^3y	10^3z
H1	68	−117	179
H2	−67	−72	179
H3	13	−305	200
H4	−117	−254	220
H5	−86	−394	102
H6	−185	−291	98
H7	44	−289	28
H8	−79	−246	−12
H11	−8 (8)	223 (7)	236 (4)
H22	65 (7)	478 (8)	178 (5)
H26	1 (7)	397 (6)	80 (4)
H33	244 (8)	275 (8)	167 (6)
H34	169 (8)	227 (8)	69 (5)
H44	148 (8)	64 (8)	104 (4)
H55	−115 (8)	125 (8)	80 (5)
H56	−61 (7)	263 (8)	38 (5)
H66	−160 (8)	367 (9)	104 (4)

[a] Hydrogen atoms bonded to carbon were not refined. All hydrogen atoms were assigned a constant isotropic temperature factor $U = 0.080$.

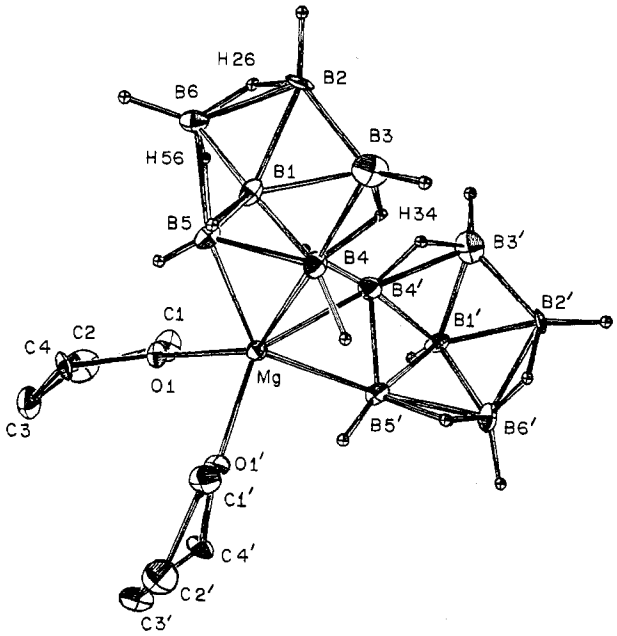

Figure 2. Molecular structure of $Mg(THF)_2(B_6H_9)_2$ showing plan views of B_6H_9 groups. Hydrogen atoms on THF rings are omitted.

ron–boron distances and boron–hydrogen distances fall within the ranges of values previously reported for boron hydrides.[22] The arrangement of each B_6 framework with respect to Mg in the structure of $Mg(THF)_2(B_6H_9)_2$ is consistent with Mg being inserted into one of the boron–boron bonds of each framework to form three-center B–Mg–B bonds. The possibility for the existence of three-center Mg–H–B bonds seems remote since the closest Mg–H distance is 2.32 (9) Å. The Mg–B distances in the B–Mg–B triangle are asymmetric, 2.38 (1) and 2.48 (1) Å, with the shorter distance being near the remaining nonbridged basal boron–boron bond in the B_6 framework. These distances are longer than the expected Mg–B single-bond distance of 2.28 Å based upon Pauling's tetrahedral radii[23] and are consistent with three-center B–Mg–B bonding in which Mg is bonded to the basal B–B edge of the B_6 polyhedron. In such a system an individual Mg–B distance is representative of a fractional bond of order less than 1. In MgB_4 which consists of chains of B_6 pentagonal pyramids with Mg atoms fitting into tunnels formed by the chains, three Mg–B distances, 2.39, 2.41, and 2.51 Å are observed.[24] Two other structures have been determined in which a non transition metal is inserted into a boron–boron bond: μ-Si-$(CH_3)_3$-1-Br-B_5H_7[25] and $[((C_2H_5)_2O)_2Cd(B_{10}H_{12})]_2$.[26] In

Table III. Bond Angles and Standard Deviations (deg) for Nonhydrogen Atoms in $Mg(THF)_2(B_6H_9)_2$

O1-Mg1-B5	103.4 (3)	O1-Mg1-B4	99.2 (3)
B4-Mg1-B5	40.4 (3)	O1-Mg1-O1′	94.0 (2)
B5-Mg1-B5′	141.8 (4)	B4-Mg1-B4′	91.4 (3)
O1-Mg1-B5′	102.4 (3)	O1-Mg1-B4′	142.4 (3)
B5-Mg1-B4′	107.8 (3)	Mg1-O1-C1	125.6 (2)
Mg1-O1-C4	124.6 (4)	C1-O1-C4	108.8 (6)
O1-C1-C2	105.0 (7)	C1-C2-C3	105.3 (8)
C2-C3-C4	105.3 (6)	O1-C4-C3	103.2 (7)
B2-B1-B6	60.1 (6)	B2-B1-B5	107.1 (7)
B2-B1-B4	102.8 (7)	B2-B1-B3	53.8 (6)
B6-B1-B5	60.5 (6)	B3-B1-B6	101.5 (7)
B4-B1-B5	57.2 (6)	B5-B1-B3	104.3 (7)
B4-B1-B6	103.8 (7)	B4-B1-B3	59.8 (6)
B1-B2-B6	58.4 (6)	B1-B2-B3	62.4 (7)
B3-B2-B6	106.9 (9)	B1-B6-B2	61.6 (6)
B1-B6-B5	60.8 (6)	B2-B6-B5	108.4 (8)
Mg1-B5-B1	132.2 (6)	Mg1-B5-B6	153.6 (7)
Mg1-B5-B4	72.9 (6)	B1-B5-B6	58.7 (6)
B1-B5-B4	60.8 (6)	B6-B5-B4	105.1 (6)
Mg1-B3-B1	127.5 (6)	Mg1-B4-B5	67.7 (5)
Mg1-B4-B3	153.8 (7)	B1-B4-B5	62.1 (6)
B1-B4-B3	60.6 (7)	B5-B4-B3	108.8 (9)
B1-B3-B4	59.6 (6)	B1-B3-B2	63.8 (7)
B2-B3-B4	110.7 (10)		

Table IV. Bond Distances and Standard Deviations (Å) for $Mg(THF)_2(B_6H_9)_2$[a]

Mg1-O1	2.019 (5)	Mg1-B5	2.382 (11)	Mg1-B4	2.478 (11)
O1-C1	1.451 (9)	O1-C4	1.450 (10)	C1-C2	1.515 (15)
C2-C3	1.469 (16)	C3-C4	1.484 (15)	B1-B2	1.784 (15)
B1-B6	1.728 (15)	B1-B5	1.766 (14)	B1-B4	1.744 (15)
B1-B3	1.762 (17)	B2-B6	1.758 (17)	B2-B3	1.603 (18)
B6-B5	1.761 (16)	B4-B5	1.679 (14)	B4-B3	1.746 (17)
B1-H11	1.15 (8)	B2-H22	1.16 (9)	B2-H26	1.25 (7)
B6-H26	1.18 (7)	B6-H66	1.11 (9)	B6-H56	1.35 (8)
B5-H56	1.24 (8)	B5-H55	0.97 (9)	B4-H44	1.13 (9)
B4-H34	1.29 (8)	B3-H34	1.30 (9)	B3-H33	1.03 (9)
Mg1-H55	2.32 (9)	Mg1-H44	2.33 (8)		

[a] The C-H bond distance is 0.98 Å.

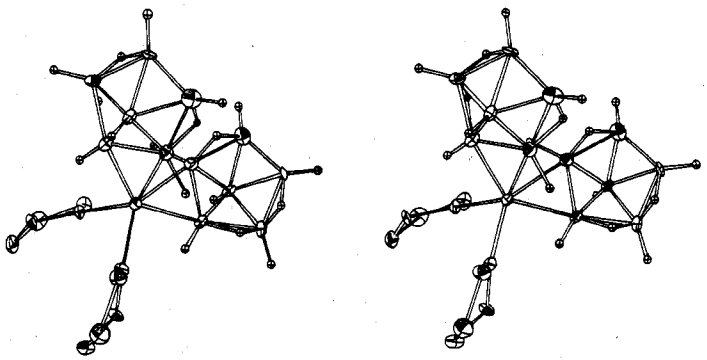

Figure 3. Stereoscopic view of $Mg(THF)_2(B_6H_9)_2$.

both cases the individual M–B distances of the B–M–B bond exceed the expected single-bond M–B distance by several tenths of an angstrom. In $[((C_2H_5)_2O)_2Cd(B_{10}H_{12})]_2$ the B–Cd–B bond is asymmetric.[26] The length of the B2–B3 bond, 1.603 (18) Å, is in good agreement with the basal boron–boron bond in B_6H_{10}.[27] The distance between the boron atoms B4–B5 which form the coordination site for Mg is 1.679 (14) Å and compares well with the boron–boron distance at the coordination site for Si in μ-$Si(CH_3)_3$-1-Br-B_5H_7,[25] 1.69 (3) Å, and Cd in $[((C_2H_5)_2O)_2Cd(B_{10}H_{12})]_2$, 1.73 (3) Å.[28] The distances between boron atoms at the metal coordination site in μ-$Fe(CO)_4$-B_7H_{12}[29] and in μ-$PtCl_2$-$(B_6H_{10})_2$[30] are 1.79 (2) and 1.82 (5) Å, respectively.

The magnesium–oxygen bond length and the bond distances and angles observed in THF are in good agreement with those obtained for other structures in which THF is coordinated to magnesium.[31] The THF rings are nonplanar with the maximum deviation of any atom from the best least-squares plane[32] being –0.195 Å for C3. Deformation of the THF rings was also found in the structure of $CH_3MgBr(THF)_3$[31a] and $MgBr_2(THF)_4$.[31c] The atoms C1, O1, and C4 are coplanar. The angle between the normals of the planes defined by C1, O1, and C4 and by C1, C2, C3, and C4 is 18°.

Preparation and Isolation of Products. Hexaborane(10) is deprotonated by dimethyl derivatives of magnesium, zinc, and cadmium in ether solvents (see eq 1 and 2, where M = Mg,

$$B_6H_{10} + (CH_3)_2M \rightarrow CH_3MB_6H_9 + CH_4 \quad (1)$$

$$CH_3MB_6H_9 \rightarrow {}^1/_2M(B_6H_9)_2 + {}^1/_2(CH_3)_2M \quad (2)$$

Zn, or Cd). The order of reactivity is $Mg(CH_3)_2 \gg Zn(CH_3)_2 > Cd(CH_3)_2 \gg Hg(CH_3)_2$ (no reaction). With $Mg(CH_3)_2$ reaction 1 is complete within 1 h at –78° in THF. The reaction of $Zn(CH_3)_2$ and of $Cd(CH_3)_2$ with B_6H_{10} in THF requires several hours for completion at temperatures in the range 0–10°. At these temperatures some decomposition of the product is noted and in the case of $Cd(CH_3)_2$ the system appears to be light sensitive as well, resulting in the deposition of some metallic cadmium. To minimize decomposition, this latter system was allowed to react in the absence of light to 80% completion. Dimethylmercury does not appear to react with B_6H_{10} in THF at temperatures up to 40°.

Methylmagnesium halides also readily abstract a proton from B_6H_{10} (see eq 3 and 4, where X = Br or I). Reactions

$$B_6H_{10} + CH_3MgX \rightarrow XMgB_6H_9 + CH_4 \quad (3)$$

$$XMgB_6H_9 \rightarrow {}^1/_2Mg(B_6H_9)_2 + {}^1/_2MgX_2 \quad (4)$$

1 and 3 proceed more rapidly in THF than in diethyl ether. In this solvent there was no evidence for nucleophilic attack on the boron framework by methide.

Attempts to isolate the species $CH_3MB_6H_9$ and $XMgB_6H_9$ from reactions 1 and 3 yielded the products shown in reactions 2 and 4. Preliminary NMR spectra[1] suggest these species may exist in solution with reactions 2 and 4 being represented as equilibria. The magnesium and zinc compounds isolated from reactions 2 and 4 were solvated: $Mg(THF)_2(B_6H_9)_2$, $Zn(THF)_2(B_6H_9)_2$. A viscous oil was produced when reaction 3 was carried out in diethyl ether using either the bromide or iodide Grignard. Addition of the THF to the ether-soluble products precipitated $Mg(THF)_2(B_6H_9)_2$.

In a 2:1 molar ratio B_6H_{10} and $Mg(CH_3)_2$ in THF undergo reaction 5. This reaction proceeds in two steps. One mole

$$2B_6H_{10} + Mg(CH_3)_2 \rightarrow Mg(B_6H_9)_2 + 2CH_4 \quad (5)$$

of methane is evolved in minutes at –78° with the formation of a heavy white precipitate. Evolution of a second mole of methane requires 6–8 h at –78° or alternatively 15 min at 0°. Crystalline $Mg(THF)_2(B_6H_9)_2$ was isolated as the sole solid product. The first step of the reaction sequence is reaction 1 above, while the second step of the sequence could involve either the reaction of B_6H_{10} with $CH_3MgB_6H_9$ or possibly disproportionation of $CH_3MgB_6H_9$ as in reaction 2 to form $Mg(B_6H_9)_2$ and $Mg(CH_3)_2$ which in turn reacts with the previously unreacted B_6H_{10}. It is not known which of these second steps is favored.

Product Stabilities and Infrared Spectra. All of the compounds reported here exhibit limited thermal and air stability. Evidence for the decomposition of $Mg(THF)_2(B_6H_9)_2$ was noted in the infrared spectrum after standing for several weeks, under vacuum, at room temperature. However, samples heated to 100° decomposed in minutes. The zinc derivative, $Zn(THF)_2(B_6H_9)_2$, was the least stable compound of the series; decomposition was significant, under vacuum, after 2–3 days at room temperature. Heating $Cd(B_6H_9)_2$ to 90° for 1 h caused no change in its infrared spectrum and it was stable for weeks, under vacuum, at room temperature.

Brief exposure of $Mg(THF)_2(B_6H_9)_2$ to air generated a strong odor of B_6H_{10}. After standing in air for 5 h the infrared spectrum of a mull of the magnesium compound displayed essentially no B–H stretch and only weak –OH absorptions. Similar air sensitivity was observed for $Zn(THF)_2(B_6H_9)_2$, but $Cd(B_6H_9)_2$ exhibited much greater stability. A 30-min exposure of powdered cadmium compound to air generated little B_6H_{10} and its infrared spectrum was unchanged except for the appearance of small peaks attributable to boric acid.

In ethereal or methylene chloride solution, $Cd(B_6H_9)_2$ and $Zn(THF)_2(B_6H_9)_2$ exhibited very limited stability. Within hours at ambient temperature the solution turned yellow and the presence of reduced metal was noted although little change was noted in the NMR spectrum. Methylene chloride and ethereal solutions of $Mg(THF)_2(B_6H_9)_2$ were stable at room temperature for days.

The infrared spectra of these compounds, which are reported in the Experimental Section, exhibit well-resolved strong bands in the B–H terminal region of 2490–2620 cm^{-1}. Broad peaks from 1800 to 2000 cm^{-1} are attributed to B–H–B absorptions. Other bands in the spectra are similar to those reported for $B_6H_9^-$ [4] or for coordinated THF.[33] The infrared spectrum

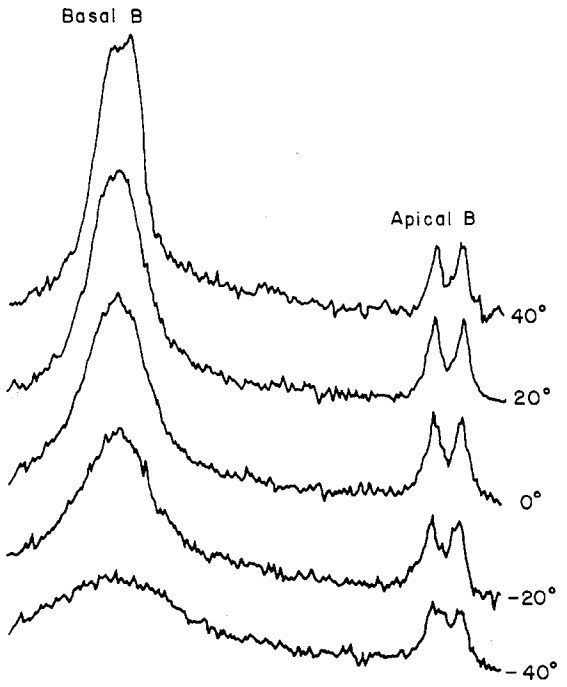

Figure 4. Boron-11 NMR spectrum of $Mg(THF)_2(B_6H_9)_2$ in CH_2Cl_2.

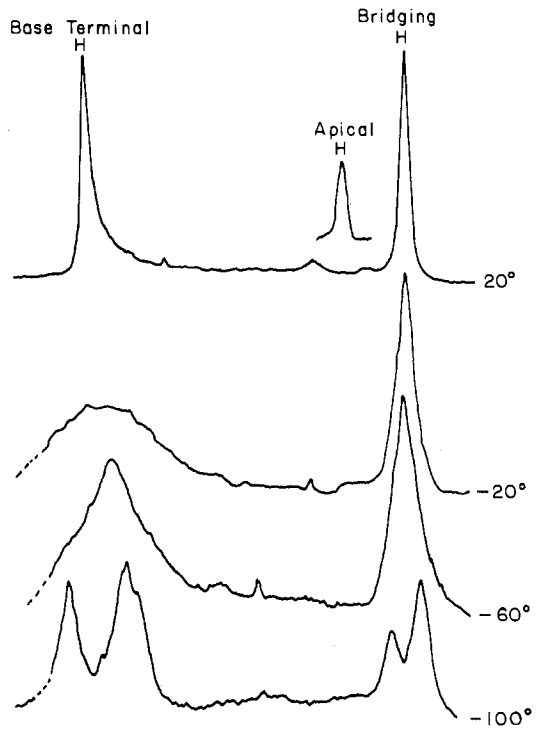

Figure 5. Proton NMR spectrum of $Mg(THF)_2(B_6H_9)_2$ in THF-d_8; basal boron-11 spin decoupled. Inset: apical boron-11 spin decoupled.

of $Cd(B_6H_9)_2$ contained only the strongest bands of coordinated THF.

Reaction of B_5H_9 with CH_3MgBr. Equimolar quantities of B_5H_9 and CH_3MgBr in THF react very slowly compared to the reaction of the Grignard with B_6H_{10}. This is consistent with the greater Bronsted acidity of B_6H_{10}.[2,3] After an initial period of 2–3 h at −23° and then 1 h at 0° only 60% of the theoretically available CH_4 had been evolved. Removal of volatile components from this system, followed by dissolving the residue in CH_2Cl_2 gave a solution which produced a boron-11 NMR spectrum which revealed the presence of $B_9H_{14}^-$ [5,34] and $B_5H_8^-$ [2] in about an equimolar ratio. The basal resonance of $B_5H_8^-$ is broader than that observed in alkali metal and tetraalkylammonium derivatives of this anion. This may be indicative of Mg interacting with the basal boron–boron bond of the anion as indicated in the boron-11 NMR spectrum of $Mg(THF)_2(B_6H_9)_2$ which is discussed below. The formation of $B_9H_{14}^-$ is consistent with earlier observations[5,35] that it is the main decomposition product of $B_5H_8^-$. When an approximately 2:1 molar ratio of B_5H_9 and CH_3MgBr was allowed to react in THF at 0° for 3 h, 65% of the theoretically available CH_4 was produced and recovery of unreacted B_5H_9 revealed that 1.8 mmol of B_5H_9 was consumed/mol of CH_4 evolved. Boron-11 NMR spectra revealed only the presence of $B_9H_{14}^-$ as a reaction product. Treatment of this system with $(CH_3)_4NCl$ permitted isolation of $(CH_3)_4NB_9H_{14}$ in 80% yield based upon the B_5H_9 consumed.

NMR Spectra. 1. $Mg(THF)_2(B_6H_9)_2$. The 32.1-MHz boron-11 NMR spectrum of $Mg(THF)_2(B_6H_9)_2$ in CH_2Cl_2 resembles that of $N(n\text{-}C_4H_9)_4B_6H_9$ in CH_2Cl_2[5] in that it consists of a low-field doublet of area 5 (δ −9.6 ppm) and a higher field doublet of area 1 (δ +49.3 ppm, J_{B-H} = 146 Hz). However, in the present case the low-field resonance is broad and the doublet is poorly resolved. Variable-temperature boron-11 NMR spectra are shown in Figure 4. Upon cooling of the sample, the peak attributed to the basal borons broadens markedly but remains symmetric in appearance. At −60° this resonance is barely discernible from the baseline. Over the temperature range studied the apical resonance shows a slight loss in resolution with decreasing temperature. This contrasts with low-temperature spectra of tetraalkylammonium and alkali metal salts of $B_6H_9^-$ which show a marked sharpening of the apical doublet with decreasing temperature.[3,5] To establish that the temperature dependence in this case is a result of the interaction of the metal with the anion, a sample of $Mg(THF)_2(B_6H_9)_2$ was briefly dissolved in CH_3CN. The solvent was then distilled from the vessel and the solid was dissolved in CD_2Cl_2. The ^1H NMR spectrum of the solution, on the basis of area ratios and chemical shifts, revealed the presence of about 2.5 mmol of coordinated CH_3CN (τ 7.65) and 0.5 mol of coordinated THF (τ 6.01 and 7.91) per $B_6H_9^-$ anion. The boron-11 NMR spectrum of this solution at ambient temperature displayed two well-resolved doublets with chemical shifts and coupling constants in excellent agreement with those observed for $N(n\text{-}C_4H_9)_4B_6H_9$. Furthermore, upon cooling this sample the same temperature dependence as in $N(n\text{-}C_4H_9)_4B_6H_9$ was observed. Acetonitrile is more basic than the anion and thus is able to compete effectively with the anion for coordination sites on the magnesium, thereby reducing the metal–B_6H_9 interaction and producing an NMR spectrum more characteristic of the free anion.

The boron-11 spin-decoupled 100-MHz ^1H NMR spectrum of $Mg(THF\text{-}d_8)_2(B_6H_9)_2$ in CD_2Cl_2 at 20° (Figure 5) displays three resonances which are assigned to the basal terminal hydrogens (τ 6.14), the apical hydrogen (τ 11.65), and the bridging hydrogens (τ 13.22). The presence of a single peak for the terminal hydrogens and a single peak for the bridging hydrogens is indicative of a dynamic system. On the basis of earlier studies of $B_6H_9^-$ [3,5] and B_6H_{10},[7] the basal terminal hydrogens are believed to be static on the NMR time scale, with their resonances being averaged through intramolecular migration of the bridging protons. Furthermore, the magnesium is believed to be involved in an exchange process at boron–boron bond sites. This, however, is probably a dissociative exchange process. If a cooperative intramolecular exchange of magnesium and bridging hydrogen occurred, bridge hydrogen resonances would probably not be averaged to a single signal.

In the particular spectrum at 20° in Figure 5 the terminal basal hydrogens are selectively decoupled from boron-11 while the apical hydrogen is undecoupled. The apical hydrogen is a quartet which was not visible at the radiofrequency transmitter power setting employed; however, it was readily visible when it was boron-11 spin decoupled (note the inset in the figure). The bridge protons show no apparent coupling with boron-11 and are therefore relatively insensitive to the boron-11 decoupling frequency employed. Though not shown in Figure 5, a point of interest is the appearance of the undecoupled basal terminal hydrogen spectrum. Instead of the expected quartet, it is a broad doublet. This represents the onset of "thermal decoupling", attributed to a rapid rate of relaxation of the boron nuclei,[36] and is consistent with the apparent absence of multiplet character of the basal boron-11 NMR spectrum (Figure 4) at 20°. From temperatures below −20°, thermal decoupling of the basal terminal protons was sufficiently effective that it was not necessary to irradiate the sample by an external power source operating at the resonance frequency of the basal boron.

As the sample is cooled below −60° (Figure 5) both the basal terminal and bridge hydrogen peaks begin to broaden and at −80° both split into a pair of peaks which are well resolved at −100°. There are two main peaks (τ 5.14 and 6.70) from the basal terminal hydrogens in an area ratio of 2:3. The larger peak has a shoulder (τ 6.9) which is reproducible in spectra of different samples of $Mg(THF\text{-}d_8)_2(B_6H_9)_2$ and suggests the presence of three basal terminal signals in the area ratio of 2:2:1. The weighted average of these three peaks (τ 6.2) agrees well with the single averaged resonance (τ 6.14) observed at higher temperatures. The bridging protons produced two peaks (τ 12.80 and 13.42) of relative areas 1:2. Their weighted average (τ 13.21) is in excellent agreement with the single averaged signal (τ 13.22) observed at higher temperatures. In contrast to that of $Mg(THF\text{-}d_8)_2(B_6H_9)_2$ the ^1H NMR spectra of LiB_6H_9 and KB_6H_9[37] display only sharp peaks for the basal terminal and bridge hydrogens down to at least −130 and −140°, respectively. Thus the presence of magnesium has a pronounced effect on the rate of hydrogen exchange on the ^1H NMR time scale.

If the ^1H NMR spectrum of $Mg(THF\text{-}d_8)_2(B_6H_9)_2$ at −100° is a limiting spectrum which effectively represents a "static" system on the ^1H NMR time scale, then it must be assumed that certain peaks in the spectrum coincidentally overlap since the spectrum implies a mirror plane of symmetry through each $Mg\text{–}B_6H_9$ moiety, while the x-ray structure reveals acentric $Mg\text{–}B_6H_9$ units (Figure 2). We prefer to believe that the spectrum is not a limiting one and that the implied mirror symmetry arises from hydrogen migration in a partially quenched system. The apparent mirror symmetry could result from migration of the three bridging hydrogens among four possible bridging sites while the magnesium is effectively fixed at a boron–boron bond. Another possibility is that the bridging hydrogens $H_{2,6}$ and $H_{3,4}$ are also effectively static while the unique bridging hydrogen is exchanging between boron–boron bonds $B_6\text{–}B_5$ and $B_4\text{–}B_5$. We favor this latter rationalization of the spectrum. (See eq 6.) Similar

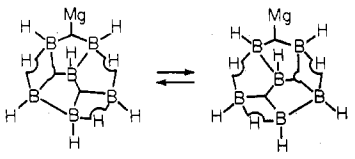

(6)

proposals, in which part of the dynamic process is said to be quenched, have been made to account for the temperature-dependent NMR spectra of $2\text{-}CH_3B_6H_9$, $2\text{-}BrB_6H_9$,[7] and $2\text{-}CH_3B_5H_7^-$.[38]

The compound $Mg(THF\text{-}d_8)_2(2\text{-}CH_3B_6H_8)_2$ produces a ^1H NMR spectrum which is also temperature dependent[39a] and can be accounted for in the same manner as the ^1H NMR spectrum of $Mg(THF\text{-}d_8)_2(B_6H_9)_2$. In the static structure the Mg is thought to be at the bridging position $B_3\text{–}Mg\text{–}B_4$ with the basal boron–boron bond $B_5\text{–}B_6$ being nonadjacent to both the $2\text{-}CH_3$ group and the magnesium. This would satisfy the observed preference of the boron–boron bond to be nonadjacent to magnesium (Figures 1 and 2) and nonadjacent to the $2\text{-}CH_3$ group.[7,39b,c]

2. $Zn(THF)_2(B_6H_9)_2$ and $Cd(B_6H_9)_2$. Variable-temperature boron-11 NMR spectra of $Zn(THF)_2(B_6H_9)_2$ and $Cd(B_6H_9)_2$ are very similar to each other over the temperature range they were studied and are also similar to boron-11 NMR spectra of $Mg(THF)_2(B_6H_9)_2$ down to about −30°. At lower temperatures asymmetries in the signals from the basal borons of $Zn(THF)_2(B_6H_9)_2$ and $Cd(B_6H_9)_2$ are observed, giving evidence for retardation of the exchange processes.

The boron-11 NMR spectrum of $Zn(THF)_2(B_6H_9)_2$ at 20° consists of a poorly resolved doublet signal from the basal borons (δ −13.2 ppm) and a sharp apical doublet (δ 48.9 ppm, $J_{B\text{–}H}$ = 138 Hz). Cooling the solution to 0° caused a broadening of the basal boron signal and it lost all indication of spin coupling with hydrogen. This peak broadened further upon continued cooling and distinct asymmetry was observed at −30°. At −50° and below, two broad peaks of approximate area 2:3 (δ −17 and −6.4 ppm) appeared.

The boron-11 NMR spectrum of $Cd(B_6H_9)_2$ at 0° consists of a poorly resolved doublet signal from the basal borons (δ −12.8 ppm) and a sharp doublet from the apical hydrogen (δ 51.3 ppm, J = 148 Hz). At −40° the basal boron signal appears as a broad symmetric hump, but asymmetry in this hump becomes evident at −50°. At −70° two broad overlapping peaks of approximate areas 2:3 appear (δ −5 and −17 ppm).

The variable-temperature ^1H NMR spectra of $Zn(THF\text{-}d_8)_2(B_6H_9)_2$ and $Cd(B_6H_9)_2$ in THF-d_8–dimethyl-d_6 ether parallel the spectra of $Mg(THF\text{-}d_8)_2(B_6H_9)_2$. However the zinc and cadmium systems appear to be quenched at higher temperatures than the magnesium system.

At 0° the boron-11 spin decoupled ^1H NMR spectrum of $Zn(THF\text{-}d_8)_2(B_6H_9)_2$ consists of a single peak from basal terminal hydrogens (τ 5.87) a single peak from bridging hydrogens (τ 12.75) and the apical hydrogen resonance (τ 11.50). Upon cooling the system, the bridge proton peak broadens and at −30° splits into two peaks of relative areas 1:2 (τ 12.45 and 13.04). Further cooling causes the peak from the basal terminal hydrogens to broaden and then split into two peaks of relative areas of about 2:3 (τ 5.33 and 6.33) at −50°. The cooling from −30 to −70° causes one of the peaks from the bridge protons to move from τ 12.45 to τ 12.60. This observation may be related to the quenching of the exchange of Zn.

At 0° the boron-11 spin-decoupled ^1H NMR spectrum of $Cd(B_6H_9)_2$ consists of a single peak from basal terminal hydrogens (τ 5.88), a single peak from bridging hydrogens (τ 12.67), and the apical hydrogen resonance (τ 11.44). Cooling the solution to −60° was required before two different peaks from basal terminal hydrogens in an area ratio of 2:3 (τ 5.15 and 6.21) could be observed. In this system bridge hydrogens do not produce two separate peaks at −60°; however a distinct shoulder is observed on the low "τ" side of the main peak which had shifted to τ 12.82.

Acknowledgment. We wish to acknowledge gratefully support of this work by the National Science Foundation. W.R.C. thanks The Ohio State University Graduate School for a Postdoctoral Fellowship.

Registry No. $Mg(THF)_2(B_6H_9)_2$, 57483-43-9; $Zn(THF)_2(B_6H_9)_2$, 57606-44-7; $Cd(B_6H_9)_2$, 57574-02-4; B_6H_{10}, 23777-80-2; $Mg(CH_3)_2$,

2999-74-8; CH_3MgBr, 75-16-1; $Zn(CH_3)_2$, 544-97-8; $Cd(CH_3)_2$, 506-82-1; B_5H_9, 19624-22-7; boron-11, 14798-13-1.

Supplementary Material Available: listing of structure factor amplitudes (4 pages). Ordering information is given on any current masthead page.

References and Notes

(1) D. L. Denton, Ph.D. Dissertation, The Ohio State University, 1973.
(2) H. D. Johnson, II, S. G. Shore, N. L. Mock, and J. C. Carter, *J. Am. Chem. Soc.*, **91**, 2131 (1969).
(3) H. D. Johnson, II, R. A. Geanangel, and S. G. Shore, *Inorg. Chem.*, **9**, 908 (1970).
(4) G. L. Brubaker, M. L. Denniston, S. G. Shore, J. C. Carter, and F. Swicker, *J. Am. Chem. Soc.*, **92**, 7216 (1970).
(5) V. T. Brice, H. D. Johnson, II, D. L. Denton, and S. G. Shore, *Inorg. Chem.*, **11**, 1135 (1972).
(6) H. D. Johnson, II, V. T. Brice, G. L. Brubaker, and S. G. Shore, *J. Am. Chem. Soc.*, **92**, 4571 (1970).
(7) V. T. Brice, H. D. Johnson, II, and S. G. Shore, *J. Am. Chem. Soc.*, **95**, 6629 (1973).
(8) V. T. Brice and S. G. Shore, *Chem. Commun.*, **1312** (1970).
(9) H. D. Johnson, II, V. T. Brice, and S. G. Shore, *Inorg. Chem.*, **12**, 689 (1973).
(10) J. H. Wotiz, O. A. Hollingsworth, and R. E. Dessy, *J. Am. Chem. Soc.*, **78**, 1221 (1956).
(11) R. R. Renshaw and O. E. Greenlaw, *J. Am. Chem. Soc.*, **42**, 1472 (1920).
(12) A. N. Nesmeyeyanov and K. A. Kocheshkov, "Series of Elemento-organic Chemistry", Vol. 3, North-Holland Publishing Co., Amsterdam, 1967, p 170.
(13) J. W. Akitt, *J. Magn. Reson.*, **3**, 411 (1970).
(14) P. W. R. Corfield and S. G. Shore, *J. Am. Chem. Soc.*, **95**, 1580 (1972).
(15) J. M. Stewart, F. A. Kundell, and J. C. Baldwin, "The XRAY System Version of 1972", Computer Science Center, University of Maryland, College Park, Md., July 1970.
(16) W. R. Clayton, M. Mangion, and E. A. Meyers, *Acta Crystallogr., Sect. A*, **28**, 743 (1975).
(17) D. T. Cromer and J. T. Waber, *Acta Crystallogr.*, **18**, 104 (1965).
(18) R. F. Stewart, E. R. Davidson, and W. T. Simpson, *J. Chem. Phys.*, **42**, 3175 (1965).
(19) D. T. Cromer, *Acta Crystallogr.*, **18**, 17 (1965).
(20) Supplementary material.
(21) C. K. Johnson, "ORTEP: A Fortran Thermal-Ellipsoid Plot Program for Crystal Structure Illustrations", USAEC Report ORNL-3694, Oak Ridge National Laboratory, Oak Ridge, Tenn., 1965.
(22) W. N. Lipscomb, "Boron Hydrides", W. A. Benjamin, New York, N.Y., 1963.
(23) L. Pauling, "The Nature of the Chemical Bond", 3rd ed, Cornell University Press, Ithaca, N.Y., 1960, p 246.
(24) R. Naslain, A. Guette, and M. Barret, *J. Solid State Chem.*, **8**, 68 (1973).
(25) J. C. Calabrese and L. F. Dahl, *J. Am. Chem. Soc.*, **93**, 6042 (1971).
(26) N. N. Greenwood, J. A. McGinnety, and J. D. Owen, *J. Chem. Soc. A*, 989 (1972).
(27) Although this distance was not reported in the original article,[26] we calculated it from the reported positional and crystal parameters.
(28) N. N. Greenwood, J. A. McGinnety, and J. D. Owen, *J. Chem. Soc.*, 989 (1972).
(29) To be published. The molecular structure has been reported: O. Hollander, W. R. Clayton, and S. G. Shore, *J. Chem. Soc., Chem. Commun.*, 604 (1974).
(30) J. P. Brennan and R. Schaeffer, *J. Chem. Soc., Chem. Commun.*, 354 (1973).
(31) (a) M. C. Perucaud and M. T. LeBilhan, *Acta Crystallogr., Sect. B*, **24**, 1502 (1968); (b) S. Toney and G. D. Stucky, *J. Organomet. Chem.*, **28**, 5 (1971); (c) M. Valino, *ibid.*, **20**, 1 (1969).
(32) H. C. Norment, "A Collection of Programs for Crystal Structure Analysis", NRL Report 5885, 1963, pp 21–23.
(33) N. N. Greenwood and N. F. Travers, *J. Chem. Soc. A*, 880 (1967).
(34) N. N. Greenwood, H. J. Gysling, J. A. McGinnety, and J. D. Owen, *Chem. Commun.*, 505 (1970).
(35) (a) G. G. Savory and M. G. H. Wallbridge, *J. Chem. Soc. A*, 179 (1973); (b) D. F. Gaines, personal communications; (c) J. H. Morris, personal communication.
(36) (a) H. Beall, C. H. Bushweller, W. J. Dewkett, and M. Grace, *J. Am. Chem. Soc.*, **92**, 3484 (1970); (b) D. Manynick and T. Onak, *J. Chem. Soc. A*, 1160 (1970).
(37) H. D. Johnson, personal communication.
(38) V. T. Brice and S. G. Shore, *Inorg. Chem*; **12**, 309 (1973).
(39) (a) R. J. Remmel, D. L. Denton, and S. G. Shore, work in preparation; (b) I. Jaworwisky, Ph.D. Thesis, The Ohio State University, 1975; (c) R. J. Remmel, Ph.D. Thesis, The Ohio State University, 1975.

Contribution from the Department of Chemistry,
Rutgers, The State University of New Jersey, Newark, New Jersey 07102

Crystal and Molecular Structure of a Nickel(II) Iodide Complex of a Macrocyclic Tetradentate Ligand[1]

ROGER A. LALANCETTE,* DOMINIC J. MACCHIA, and WILLIAM F. FUREY

Received August 11, 1975 AIC50601T

The crystal structure of $Ni(C_{20}H_{22}N_2O_4)I_2$ has been determined by single-crystal x-ray diffraction using automatic diffractometer methods to collect three-dimensional data. The structure was solved using the Patterson heavy-atom technique and Fourier difference electron density maps and was refined by full-matrix least-squares methods to a conventional residual $R_F = 0.038$ and a weighted residual $R_w = 0.046$ based on 2686 reflections with $I_{obsd} \geq 3\sigma(I)$. The compound crystallizes in the orthorhombic space group $Pna2_1$ with cell dimensions of $a = 20.931$ (8) Å, $b = 14.221$ (3) Å, $c = 7.478$ (1) Å, and $V = 2226$ (1) Å^3. The density calculated assuming $Z = 4$ is 1.99 g cm^{-3} as compared with a measured density of 2.00 g cm^{-3}. The structure consists of discrete molecules; the two iodine atoms lie in cis-coordination sites, the two oxygen atoms lie trans to one another, and the two nitrogens lie cis to one another in the inner coordination sphere. The Ni–I bond distances of 2.711 (1) and 2.757(1) Å are consistent with the calculated sum of the covalent radii for octahedral Ni(II) complexes.

Introduction

Kluiber and Sasso[2a] have reported that bis(*N*-2-bromoethylsalicylaldiminato)nickel(II) reacts with sodium iodide in acetone to form a paramagnetic complex of empirical formula $Ni(C_{18}H_{18}N_2O_2)I_2$. The structure of this red material was reported by Johnston and Horrocks[2b] and shows the complex to be octahedral with the two iodides in trans configuration, the two oxygens in trans configuration, and the two nitrogens also in trans configuration. This tetradentate macrocyclic imine–ether complex is essentially planar with the iodine atoms above and below the plane.

Kluiber and Sasso[3] have also made nickel complexes with various substituents on the ligand. When a methoxy group is inserted in the para position to the ether oxygen in the salicylaldimine ligand and the nickel(II) complex is allowed to form at room temperature, a green compound crystallizes from acetone solution. If the ligand and metal are allowed to react in boiling acetone (56 °C), then two green crystalline modifications can be isolated from the solution: hexagonal crystals and rhombic crystals.

Elemental analysis of either modification yielded the following values. Anal. Calcd for $Ni(C_{20}H_{22}N_2O_4)I_2$: C, 36.02; H, 3.32; N, 4.20. Found: C, 36.15; H, 3.57; N, 4.01.

This study was undertaken to determine if the rhombic and